ACS MATERIALS Au
AN OPEN ACCESS JOURNAL OF THE AMERICAN CHEMICAL SOCIETY

pubs.acs.org/materialsau Letter

Growth of Graphene on a Liquified Copper Skin at Submelting Temperatures

Hadi Arjmandi-Tash and Grégory F. Schneider*

Cite This: *ACS Mater. Au* 2022, 2, 79–84 Read Online

ACCESS | Metrics & More | Article Recommendations | Supporting Information

ABSTRACT: In chemical vapor deposition of graphene, crossing over the melting temperature of the bulk catalyst is an effective approach to heal the defects and thus improve the crystallinity of the lattice. Here, electromagnetic absorption (the capability of metals to absorb radiated thermal energy) yields a thin skin of liquid metal catalyst at submelting temperatures, allowing the growth of high quality graphene. In fact, a chromium film initially deposited on one side of a copper foil absorbs the thermal energy radiated from a heating stage several times more effectively than a plain copper foil. The resulting migration of the chromium grains to the other side of the foil locally melts the copper, improving the crystalline quality of the growing graphene, confirmed by Raman spectroscopy. The process duration is therefore dramatically minimized, and the crystallinity of the graphene is maximized. Remarkably, the usual annealing step is no more necessary prior to the growth which together with unlocking the direct healing of defects in the growing graphene, will unify growth strategies between a range of catalysts.

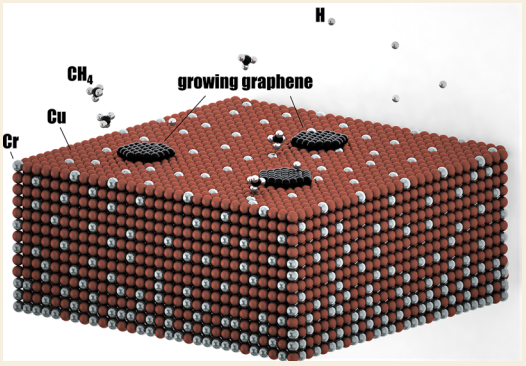

KEYWORDS: *graphene, chemical vapor deposition, electromagnetic absorption, chromium, liquid metal catalyst, cold-wall chambers*

INTRODUCTION

The chemical vapor deposition (CVD) of graphene is in general performed in tube oven (= "hot-wall") chambers[1−5] with the heating element placed outside the chamber. Symmetrical thermal radiation forms a uniform thermal zone in which the specimen (e.g., a copper foil) receives a homogeneous heat flux (= absorbed thermal energy per unit area and time) from surroundings. The heating in "cold-wall chambers"[6−10] is heterogeneous: the heating stage is placed inside the chamber which directly heats up the specimen via thermal conduction. The process involves a large thermal gradient between the stage (normally at $T > 1000$ °C) and the walls (normally at $T \sim 100$ °C) which eventually provides a nonuniform heating zone which can potentially lead to random growth. Although the graphene growth in cold-wall chambers is cost effective, the directional heating is a major drawback.

Mixing (alloying) metals is an effective approach to combine the favorable properties of different metals for specific applications. Particularly, nickel and molybdenum were rationally alloyed to achieve a self-limited growth of graphene with outstanding reproducibility.[11] In fact, the precipitated carbon species form strong and stable bonds with molybdenum and are excluded from the growth to yield strictly single-layer graphene. Separately, monolayer graphene has been achieved by suppressing multilayer formation via covering the active sites on cobalt surface by a copper film.[12] The catalytic capability of copper was also dramatically improved by alloying with nickel;[13] Indeed the nickel-mediated segregation of carbon radicals in the copper−nickel alloy increases the growth rate by an order of magnitude over singular copper.

Growth of graphene on liquid catalyst (e.g., copper) is advantageous:[14] Crystalline defects (including grain boundaries) and the surface roughness, as the potential graphene nucleation sites, are negligible when the catalyst is in liquid phase favoring monolayer graphene growth.[15] In a special regime in the presence of adsorbates on the liquid subphase, though, a complex flow pattern may generate isolated and distinguished domains/cells on liquid surface.[16] Formulated by the Benard−Marangoni effect, this flow pattern is a result of the solutal or thermal instabilities driven by adsorbate-related variations in surface tension which eventually would challenge the synthesis of continuous, uniform graphene.[17] In either case, however, the mobile catalytic atoms on the liquefied subphase lower the amount of defects in the graphene crystal lattice (e.g., voids) by driving a so-called "defect healing" process in which pentagonal and heptagonal carbon rings convert to hexagons.[18] Indeed, by using appropriate supporting layers to prevent the dewetting of the copper foil, epitaxial growth of

Received: September 16, 2021
Revised: December 8, 2021
Accepted: December 8, 2021
Published: December 17, 2021

https://doi.org/10.1021/acsmaterialsau.1c00047
ACS Mater. Au 2022, 2, 79–84

single-crystal domains of ~200 μm has been realized above the melting temperature of copper.[14]

In this paper, we grow graphene on a bicomponent substrate composed of copper and chromium, respectfully with outstanding catalytic properties and electromagnetic absorption. The backside of a copper foil is initially covered with a thin chromium film which enables the absorption of thermal energy radiated from the hot plate in a cold-wall chamber, well beyond the bare copper foil. The chromium film transforms into hot nanorodes and migrates through the foil to the other side, where graphene is to be grown. The process includes local melting of the copper which enables defect healing of the growing graphene. A continuous high-quality graphene sheet is achieved in only 5 min, nominating the protocol as one of the shortest ever reported. From the materials science perspective, we identify an original strategy for mixing materials which is largely distinct from conventionally known scenarios for alloying metals.

EXPERIMENTAL SECTION

Cold-wall chambers has been continuously optimized to grow high quality graphene. In fact, recent progresses demonstrated that, with an optimized recipe, a cold-wall chamber is capable of producing graphene with the quality comparable to that of the conventional hot-wall chamber.[6,10,12,19] For the purpose of this project, however, we have started with an unsuccessful recipe, including subsequent annealing and growth phases (detailed in the Methods section in the Supporting Information), and demonstrate that the inclusion of the chromium to the copper foil considerably improves the outcome via an unprecedented mechanism. The experiments are done on a copper foil (Alfa Aesar, 99.999% purity, 25 μm thickness) on which a chromium film of 50 nm was initially evaporated. We placed the sample on the hot stage of a cold-wall CVD setup (nanoCVD-8G, Moorfield Nanotechnology) with the chromium-deposited side facing the stage (we will refer to this side as the "bottom side" throughout this paper; see the schematic in the inset of Figure 1a). The growth temperature and the annealing duration were varied at different experiments (explained in the following), but the growth duration was fixed at 3 min. With an annealing duration of 7 min at 1035 °C, chromium migrates to the top side where the graphene grows during the growth phase. Figure 1a displays the top side of a copper foil initially and partially covered with a chromium film at the bottom left side (see the inset schematic). The right side of the sample (with no chromium film deposited) appears shiny and smooth; the migration of the chromium film to the top side, however, turns the sample matte (rough) on the left side. High-resolution atomic force microscopy (AFM, Figure 1b also inset of Figure 3a) and scanning electron microscopy (SEM, Figure 1c and d) show that the diffusion of the chromium has induced a complex microstructure at the surface of the foil: The surface has split into a landscape of two phases where a lath structure with sharp edges pops out from the background layer (Figure 1b and c). Next, a standard copper etching solution (ammonium persulfate) is used to dissolve the background copper while the lath structure is dissolved in a chromium etcher (Supporting Information). The experiment implies that copper remains the major constituent of the background while the lath structure mainly consists of chromium (although a trace amounts of one element in another is possible).

We characterized the quality of the grown graphene by means of Raman spectroscopy (Figure 1e). In agreement with our earlier publication,[10] the unoptimized growth recipe provides poor-quality graphene (or even amorphous carbon) on the plain copper. The graphene grown on the Cu/Cr, however, exhibits standard Raman peaks (G peak at ~1580 cm^{-1} and 2D peak at ~2680 cm^{-1}) and is of superior crystalline quality, as evidenced by a negligible D peak (at 1350 cm^{-1}).

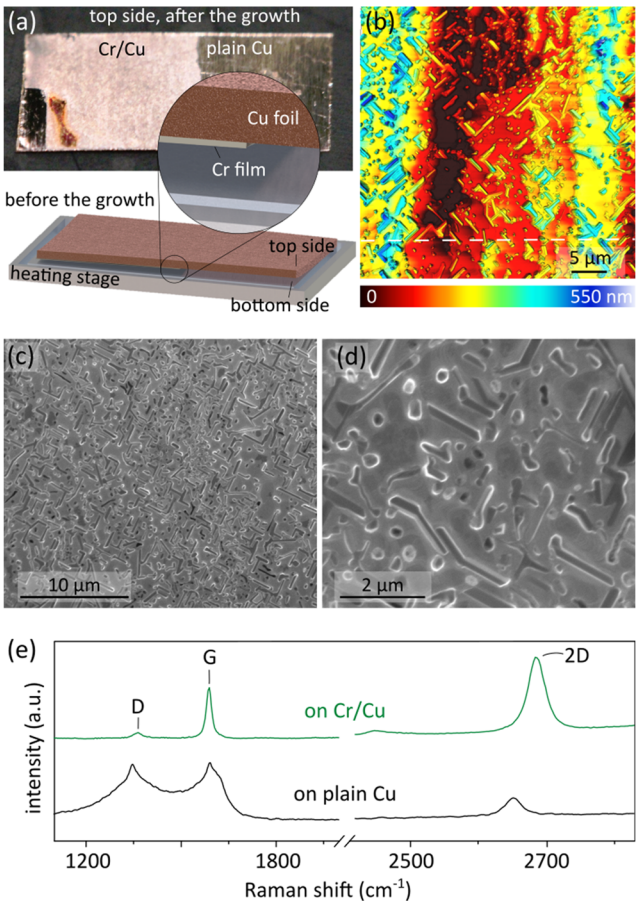

Figure 1. Graphene grown on a chromium−copper system. (a) Optical micrograph of a test sample (2 cm × 1 cm) after the growth of graphene: the bottom side of the copper foil (facing the heating stage) was initially covered with a thin (~100 nm) chromium film (demonstrated in the inset). During the growth, chromium migrates to and makes the top surface rough. (b) Representative atomic force micrograph featuring chromium texture popped out from the copper background on the left side of the sample in (a). (c, d) Representative low- and high-magnification scanning electron micrographs of the left side of the sample in (a). (e) Comparison of the Raman spectroscopy of the graphene grown on the left (on Cr/Cu) and right (plain Cu) sides of the sample in (a).

Figure 2 provides an in-depth Raman characterization of the sample after the growth of graphene. The migration of the chromium from the bottom to the top side is evident in the optical micrograph in Figure 2a. We identified low-frequency Raman spectral bands which are sensitive to the chemical constituents of the substrate. The chromium phase manifests itself as a strong peak centered at 85 cm^{-1} and is distinct from the background copper with a low-amplitude signature at its right shoulder (inset of Figure 2a, and Figure 2b and c). Two-dimensional mappings of the Raman characteristic peaks of graphene are provided in panels (d)−(f). The narrow 2D peak (fwhm <50, panel d) and large I_{2D}/I_G ratio (>1, panel e) are the signatures of monolayer graphene.[20] The graphene is of pronounced crystalline quality as evidenced by a negligible I_D/I_G ratio (panel f). Interestingly, the properties of the graphene are independent of the local structure (texture) of the underlying substrate as no correlation between the mappings in (d, e, f) and (b) is observed. This is important evidence to explain the migration of the chromium, and the improved quality of the graphene which will be discussed later.

The migration of the chromium from the bottom to the top side of the copper foil starts during the annealing phase of the growth. Figure 3a correlates the Raman spectra and the surface morphology of several samples having gone through a graphene growth cycle at 1035 °C, but

https://doi.org/10.1021/acsmaterialsau.1c00047
ACS Mater. Au 2022, 2, 79−84

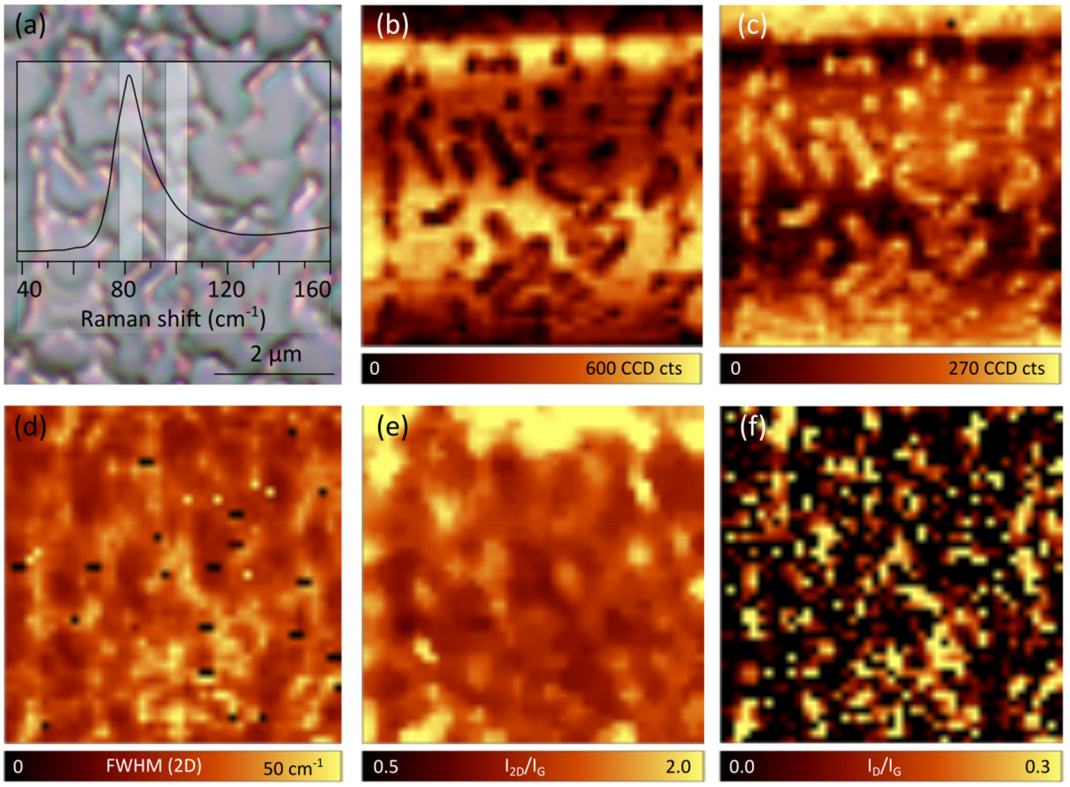

Figure 2. Raman characterization of graphene on chromium−copper system. (a) Optical micrograph of a selected window featuring chromium structures migrated to the front side of the Cu foil after 10 min of growth (7 min of annealing) at 1035 °C. The inset shows a low-frequency peak sensitive to the Cr/Cu composition in the Raman spectrum. (b) Mapping the amplitude of the Raman signal at the narrow band centered at 100 cm^{-1} (see the spectrum in (a)). The band corresponds to the copper background. (c) Mapping the amplitude of the Raman signal at the narrow band centered at 85 cm^{-1}. The band corresponds to the chromium microstructures. (d) Mapping the width of the graphene Raman 2D peak (centered at ∼2680 cm^{-1}): The width of the 2D peak hardly exceeds 50 cm^{-1}, manifesting that the graphene is predominantly monolayer. (e) Mapping the relative intensity of the 2D (I_{2D}) and G (I_G, centered at ∼1580 cm^{-1}) peaks: The I_{2D}/I_G ratio stays mainly above one as another indication of monolayer graphene. (f) Mapping the relative intensity of the D (I_D, centered at ∼1350 cm^{-1}) and G peaks: The I_D/I_G ratio stays close to zero indicating a negligible amount of crystalline defects.

with varied annealing durations. The growth duration (after the annealing) is set to 3 min for all the experiments here. Annealing durations below 6 min (i.e., the total process duration of less than 9 min) have negligible effect on the surface corrugations of the foil and are insufficient to have the chromium migrated to the top side. Here, the growth process is similar to conventional approaches with an insufficient (too short) copper annealing phase leading to a poor graphene quality, manifested by a considerably large-amplitude D peak. Chromium traces start to appear in the sample with the total process duration of 10 min (referred to as the optimized process duration, t^*). Graphene quality is the highest in a tight "temporal window" ($\Delta t^* \sim 1$ min at 1035 °C) close to t^*. Longer process (annealing) durations, however, degrade the graphene.

The optimized process duration depends on how fast chromium migrates to the top side of the copper foil which itself is a strong function of the process temperature. Figure 3b plots t^* at various growth temperatures, depicting a linear correlation between 1005 °C and 1045 °C. Interestingly, while a minimum total process duration of $t^* > 20$ min (with $\Delta t^* = 6$ min) minimizes the crystalline defects at 1005 °C, the process could be as short as 5 min (2 min of annealing followed by 3 min of the growth) to achieve a decent graphene quality at 1045 °C. The allowed temporal window is tighter at elevated temperatures. Increasing the growth temperature above 1045 °C does not affect t^* and Δt^* considerably. The minimum growth duration of 5 min is one of the shortest ever reported to achieve a continuous graphene layer.[12]

Two unexpected observations were identified in this work, namely, (a) the migration of the chromium from the back to the front side of the copper foil and (b) the improved quality of the graphene in the presence of the chromium. The rest of this paper seeks appropriate mechanisms to explain these observations. Few mechanisms might be considered to explain the chromium migration: (i) Mixing of the chromium and copper to form a conventional binary alloy is a potential scenario. The operation temperature of the CVD setup, however, remains below the solidus line in the chromium−copper phase diagram (1076 °C[21]), illustrating that the conventional alloying process, including mixing of molten components, is irrelevant here. (ii) Random thermal motion of the materials, formulated by the Fick's law of diffusion[22] (including grain boundary and lattice diffusion[23]), on the other hand, should be independent of the placement of the sample with respect to the heating stage and would eventually result in a uniform concentration across the foil. The chromium film in our experiments, however, migrates through the copper solely when it initially faces the heating stage and is specific to cold-wall chambers: Indeed similar thermal processes with flipped samples (chromium film initially facing up) or inside a tube-oven chamber (instead of a cold-wall chamber) did not cause the migration of the chromium (Supporting Information). X-ray photoelectron spectroscopy (XPS) analysis of the samples, furthermore, revealed that the concentration of the chromium in the top side of the foil exceeds 40% right after t^* (Figure 3c); in fact, the governing mechanism in our system shifts a high concentrated chromium region from one side to the other side of the foil. (iii) Thermal diffusion of solids in which a temperature gradient energizes a material of a certain thermodiffusion coefficient to diffuse, might explain the directionality of the observation: in contrast to the tube-oven chambers which provide a uniform heating zone, there is a large thermal gradient between the heating stage ($T >$ 1000 °C) and the walls (∼100 °C) in cold-wall reaction chambers. A

https://doi.org/10.1021/acsmaterialsau.1c00047
ACS Mater. Au 2022, 2, 79−84

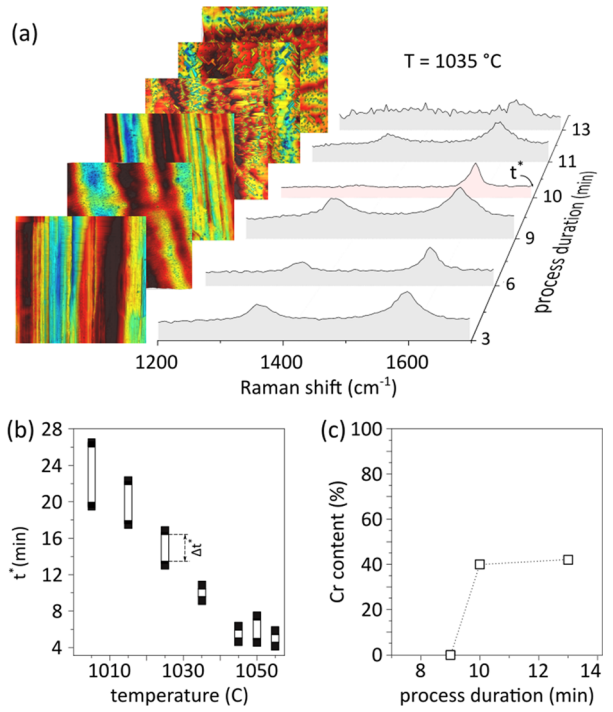

Figure 3. Quality of the graphene as a function of process duration. (a) Raman spectra of several graphene samples grown with different process durations, ranging from 3 min to 13 min (annealing duration ranging from 0 min to 10 min); t^* marks the optimum process duration which provides the lowest D peak (highest crystalline quality). The inset figures on the left show the surface morphology of the corresponding samples, mapped by AFM. The color code ranges between 0 nm and 600 nm. (b) Optimum process duration (t^*) of different samples as a function of the growth temperature. Δt^* (open rectangular markers) corresponds to the temporal window over which the graphene quality is the highest. Filled markers correspond to uncertain regions in between subsequent samplings. (c) Chromium content as a function of the process duration estimated by X-ray photoelectron spectroscopy (XPS) at the top surface of the foil.

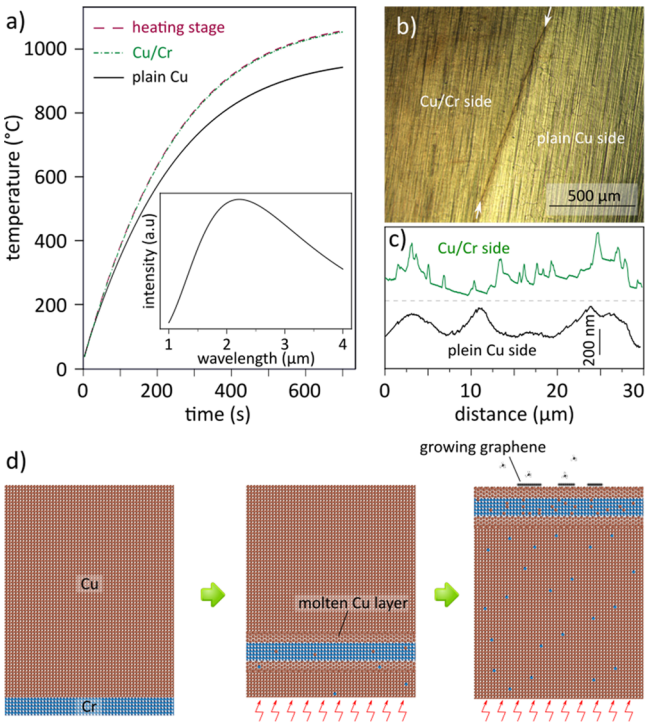

Figure 4. Potential scenario explaining the migration of the chromium accompanied by improved graphene quality. (a) Simulation of the temperature of the heating stage, chromium-coated and plain copper foil upon powering up the resistive heater. Inset: blackbody radiation spectrum at 1035 °C, formulated by Planck's equation.[34] (b) Optical micrograph focusing at the border of the Cr/Cu and plain Cu sides after 10 min of the growth process at 1035 °C. A groove appears and splits the two sides, marked by white arrows. (c) Representative surface profiles over the Cr/Cu (corresponding to the dashed line in Figure 1b) and plain Cu sides; horizontal axis shows the distance on the samples over which that AFM data is measured. (d) Our proposed mechanism explaining the migration of the chromium from the bottom to the top sides of the copper foil: The chromium film absorbs electromagnetic energy radiated by the hot stage at the elevated temperatures and partially melts the neighboring layers of the copper foil. The chromium film moves up through the molten copper; with an appropriate timing, the growth of the graphene occurs on the molten copper layers, with an improved crystalline quality.

naive hypothesis may consider that the foil "feels" this thermal gradient, causing the chromium atoms to diffuse from the hotter side (facing the heater) to the colder side (facing the cold wall, in contact with the fresh operation gases) of the copper foil, but not in the reverse direction. Our finite element simulations, however, rules out this scenario, as the high thermal conductivity of copper results in a negligible temperature gradient between its faces (Supporting Information).

The observation of improving graphene quality in the presence of the chromium is also unprecedented. Basic scenarios including chromium assisting to scavenge oxygen from possible leaks in the system are irrelevant as in the same setup, the growth of graphene with decent quality on bare copper foil (no chromium) is possible, albeit with some structural modifications.[10] Separately, no catalytic property of chromium in the CVD of graphene has been reported so far; instead chromium has been used to block the graphene growth on copper foil[24] to achieve patterned graphene. Furthermore, the degradation of the graphene quality after t^* (Figure 3a) with saturated chromium density (Figure 3c) rules out any possible cocatalytic activity of chromium (as was reported for the CVD of carbon nanotubes[25]).

Any successful scenario explaining our observations has to be built up based on two important facts. First, at the elevated operation temperature, the heating stage acts as a (semi-) blackbody radiator, emitting electromagnetic waves in the near-infrared spectrum (inset Figure 4a). Copper is a reflective material in this spectral range, exhibiting a negligible electromagnetic absorption of 7% at elevated temperatures.[26] Chromium, however, exhibits an electromagnetic absorption of ~40%.[27] In other words, while uncoated copper reflects back some 93% of incoming radiation, chromium coating dramatically improves radiative heat transfer by almost 6 folds. Thermal conduction remains a parallel heat transfer mechanism yet. We modeled the heat flow inside the oven considering thermal convection (by the process gases) and radiation to the cold walls (Figure 4a; see the Supporting Information for the details of modeling). Interestingly, by powering up the heater, the temperature of the uncoated copper foil falls below that of the stage by ~100 °C. Note that the quality of chemically synthesized graphene is highly sensitive to the reaction temperature as insufficient heating fails to provide the necessary activation energy to decompose the precursors.[28] Indeed this temperature difference between the foil and the stage explains the typically seen poor quality of graphene in cold-wall chambers.[3,10] The improved thermal energy absorption, however, drives the chromium-coated copper foil to follow the temperature of the heating stage closely. The higher "effective" growth temperature, however, is not the solitary origin of the increased graphene quality on the chromium-coated copper foil.

As another important fact, two observations demonstrate that the migration of the chromium is accompanied by the local melting of the

https://doi.org/10.1021/acsmaterialsau.1c00047
ACS Mater. Au 2022, 2, 79−84

copper foil. Generation of grooves between the Cr/Cu and plain Cu sides (Figure 4b) is the first evidence, which could be explained by considering a molten phase in contact with the solid copper phase during the operation: indeed the transformation of the melt (lower density, thus higher volume) to solid (higher density, thus lower volume) during the cool down period comes with a shrinkage in the volume, causing a groove.[29] It is worth noting that similar grooves are typically seen at the melt/mold interface after solidifying a molten metal in casting processes.[30] The second evidence appears by comparing the morphology of the foils with and without chromium (Figure 4c): The plain copper side features gradual undulations of the surface which is a result of the specific fabrication process of the foil.[31] Migrated chromium, on the other hand, forms evident mesas of ∼80 nm amplitude. Interestingly, the surface of the copper between the chromium mesas has been flattened, which would be possible only after a melting process.

Chromium-assisted melting of copper is the major cause of the improvement in graphene crystalline quality in our experiments: In fact the higher mobility and longer surface-diffusion range of the molten copper atoms drive a "defect healing" process in which the structural defects (e.g., pentagons and heptagons) transform into perfect hexagonal rings, as observed by quantum-chemical molecular dynamics simulations.[18] The effect would be amplified by the improved diffusive mobility of the carbon species on the surface. Experimentally, defect-free graphene achieved by CVD has already been demonstrated on molten copper foils.[14,15,32]

We now propose a potential mechanism to explain our observations: Chromium deposited on the bottom side of the copper absorbs electromagnetic radiation, well beyond the plain copper, and starts melting neighboring layers of the copper foil (Figure 4d, left). Melting the copper opens up pathways for the migration of chromium species to the top surface (Figure 4d, middle). With optimized timing, the growth of graphene would start when a thin layer on the surface of the copper foil is in the molten state but chromium has not reached the surface yet (Figure 4d, right). In this case, the chromium reaches the top surface close to the end of the growth process and thus the local quality of graphene (e.g., Raman signatures) is independent of the features on the foil (refer to the discussion in Figure 2). In a delayed process ($t^* > 10$ min in Figure 3a), however, the presence of the noncatalyst chromium on the surface degrades the graphene quality. The rate of advancing the chromium front scales inversely with the temperature, explaining the longer t^* and Δt^* measured at lower temperatures (Figure 3b).

We note that the improved radiation absorption by the chromium cannot directly cause the melting of the copper foil as the temperature of the heating stage remains below the melting point of copper. In particular, we noticed the migration of the chromium at temperatures as low as 870 °C (∼200 °C below the melting point of copper). The surface melting phenomenon[18,29] in which a thin layer (typically of few nanometer thickness) at the surface melts below the melting point of the bulk is an important consideration. In fact, the reduced coordination degree of surface atoms is behind this advanced melting: Expressed by the Lindemann criterion,[33] cohesive energy associated with the bonding between the atoms in a crystalline state determines the melting temperature of a solid. This energy is lower for the atoms close to the surface, as a result of the fewer bonds they can make with neighboring atoms, causing a lowered melting temperature. Note that a reduction of 25% in the melting temperature (compared to bulk melting temperature) has been observed at the surface of a lead specimen.[29] The same phenomenon could occur at the Cu/Cr interface in this work, though in the absence of a robust experimental/theoretical demonstration, this scenario yet remains a potential hypothesis.

CONCLUSIONS

We introduce an unprecedented approach in the chemical vapor deposition of graphene in which the migration of a chromium film—initially deposited on the back side of a copper foil—to the front side causes the local melting of the foil and eventually improves the quality of the growing graphene. A continuous graphene sheet now is grown in less than 5 min, as in the presence of the molten phase, the thermal annealing step in conventional CVD recipes is no longer required. We investigate the mechanism driving the chromium species through the copper. Our report introduces the electromagnetic absorption as an efficient knob in the scalable CVD growth of high-quality graphene. The findings in this report promote the science of metal mixing.

ASSOCIATED CONTENT

Supporting Information

The Supporting Information is available free of charge at https://pubs.acs.org/doi/10.1021/acsmaterialsau.1c00047.

Details of the process (preparation of the substrate, recipe of the chemical vapor deposition, characterization of the grown graphene), along with simulation of the temperature field in the chamber and modeling of the heat transfer to the specimen in the oven (PDF)

AUTHOR INFORMATION

Corresponding Author

Grégory F. Schneider − *Faculty of Science, Leiden Institute of Chemistry, Leiden University, 2333CC Leiden, The Netherlands;* orcid.org/0000-0001-5018-3309; Email: g.f.schneider@chem.leidenuniv.nl

Author

Hadi Arjmandi-Tash − *Faculty of Science, Leiden Institute of Chemistry, Leiden University, 2333CC Leiden, The Netherlands;* orcid.org/0000-0002-2800-8659

Complete contact information is available at: https://pubs.acs.org/10.1021/acsmaterialsau.1c00047

Notes

The authors declare no competing financial interest.

ACKNOWLEDGMENTS

The work leading to this paper has gratefully received funding from the European Research Council under the European Union's Seventh Framework Programme (FP/2007-2013)/ERC Grant Agreement No. 335879 project acronym "Biographene", and The Netherlands Organisation for Scientific Research (Vidi 723.013.007). The authors acknowledge Dr. Irene Groot (Leiden University) for useful discussions about the background science and also for her valuable feedbacks on preparing the manuscript. The authors also acknowledge Frank de Pont (Comsol BV) for the simulation of the system, discussed in the Supporting Information section S3.

REFERENCES

(1) Li, X.; et al. Large-area synthesis of high-quality and uniform graphene films on copper foils SOI. *Science* **2009**, *324* (5932), 1312−4.

(2) Li, X.; et al. Large-Area Graphene Single Crystals Grown by Low-Pressure. *J. Am. Chem. Soc.* **2011**, *133* (9), 2816−9.

(3) Han, Z.; et al. Homogeneous Optical and Electronic Properties of Graphene Due to the Suppression of Multilayer Patches During CVD on Copper Foils. *Adv. Funct. Mater.* **2014**, *24* (7), 964−970.

(4) Arjmandi-Tash, H.; et al. Large scale graphene/h-BN heterostructures obtained by direct CVD growth of graphene using

high-yield proximity-catalytic process. *J. Phys. Mater.* **2018**, *1* (1), 015003.
(5) Arjmandi-Tash, H. In situ growth of graphene on hexagonal boron nitride for electronic transport applications. *J. Mater. Chem. C* **2020**, *8*, 380−386.
(6) Bointon, T. H.; Russo, M. D.; Barnes, S.; Craciun, M. F. High Quality Monolayer Graphene Synthesized by Resistive Heating Cold Wall Chemical Vapor Deposition. *Adv. Mater.* **2015**, *27* (28), 4200−4206.
(7) Neves, A. I. S.; et al. Transparent conductive graphene textile fibers. *Sci. Rep.* **2015**, *5*, 9866.
(8) Miseikis, V.; et al. Rapid CVD growth of millimetre-sized single crystal graphene using a cold-wall reactor. *2D Mater.* **2015**, *2* (1), 014006.
(9) Mishra, N.; Miseikis, V.; Convertino, D.; Gemmi, M.; Piazza, V.; Coletti, C. Rapid and catalyst-free van der Waals epitaxy of graphene on hexagonal boron nitride. *Carbon* **2016**, *96*, 497−502.
(10) Arjmandi-Tash, H.; Lebedev, N.; van Deursen, P.; Aarts, J.; Schneider, G. F. Hybrid cold and hot-wall chamber for fast synthesis of uniform graphene. *Carbon* **2017**, *118*, 438−442.
(11) Dai, B.; et al. Rational design of a binary metal alloy for chemical vapour deposition growth of uniform single-layer graphene. *Nat. Commun.* **2011**, *2* (May), 522.
(12) Sugime, H.; et al. Low temperature growth of fully covered single-layer graphene using a CoCu catalyst. *Nanoscale* **2017**, *9* (38), 14467−14475.
(13) Wu, T.; et al. Fast growth of inch-sized single-crystalline graphene from a controlled single nucleus on Cu−Ni alloys. *Nat. Mater.* **2016**, *15*, 43−47.
(14) Wu, Y. A.; et al. Large Single Crystals of Graphene on Melted Copper Using Chemical Vapor Deposition. *ACS Nano* **2012**, *6* (6), 5010−5017.
(15) Geng, D.; et al. Uniform hexagonal graphene flakes and films grown on liquid copper surface. *Proc. Natl. Acad. Sci. U. S. A.* **2012**, *109* (21), 7992−7996.
(16) Paronyan, T. M.; Pigos, E. M.; Chen, G.; Harutyunyan, A. R. Formation of ripples in graphene as a result of interfacial instabilities. *ACS Nano* **2011**, *5* (12), 9619−9627.
(17) Harutyunyan, A. R. Uniform hexagonal graphene film growth on liquid copper surface: Challenges still remain. *Proc. Natl. Acad. Sci. U. S. A.* **2012**, *109* (31), E2099.
(18) Li, H.-B.; et al. Graphene nucleation on a surface-molten copper catalyst: quantum chemical molecular dynamics simulations. *Chem. Sci.* **2014**, *5* (9), 3493−3500.
(19) Sarno, M.; Rossi, G.; Cirillo, C.; Incarnato, L. Cold Wall Chemical Vapor Deposition Graphene-Based Conductive Tunable Film Barrier. *Ind. Eng. Chem. Res.* **2018**, *57* (14), 4895−4906.
(20) Ferrari, a C.; et al. Raman Spectrum of Graphene and Graphene Layers. *Phys. Rev. Lett.* **2006**, *97* (18), 187401.
(21) Zeng, K.; Hämäläinen, M. Thermodynamic analysis of stable and metastable equilibria in the Cu-Cr system. *CALPHAD: Comput. Coupling Phase Diagrams Thermochem.* **1995**, *19* (1), 93−104.
(22) Gupta, D., Ed. *Diffusion Processes in Advanced Technological Materials*; Springer-Verlag: Berlin, Heidelberg, 2005.
(23) German, R. M. Thermodynamic and Kinetic Treatments. In *Sintering: from Empirical Observations to Scientific Principles*; Butterworth-Heinemann, 2014.
(24) Hurch, S.; Nolan, H.; Hallam, T.; Berner, N. C.; McEvoy, N.; Duesberg, G. S. Inkjet-defined field-effect transistors from chemical vapour deposited graphene. *Carbon* **2014**, *71*, 332−337.
(25) HunHan, J.; Yoo, J.-E. Low Temperature Synthesis of Carbon Nanotubes by Thermal ChemicalVapor Deposition Using Co-Catalyst. *J. Korean Phys. Soc.* **2001**, *39*, S116−S119.
(26) Setién-Fernández, I.; Echániz, T.; González-Fernández, L.; Pérez-Sáez, R. B.; Tello, M. J. Spectral emissivity of copper and nickel in the mid-infrared range between 250 and 900 °C. *Int. J. Heat Mass Transfer* **2014**, *71*, 549−554.
(27) Johnson, P.; Christy, R. Optical constants of transition metals: Ti, V, Cr, Mn, Fe, Co, Ni, and Pd. *Phys. Rev. B* **1974**, *9* (12), 5056−5070.
(28) Zhang, Y.; Zhang, L.; Zhou, C. Review of chemical vapor deposition of graphene and related applications. *Acc. Chem. Res.* **2013**, *46*, 2329−2339.
(29) Pakhnevich, A. A.; Golod, S. V.; Prinz, V. Y. Surface melting of copper during graphene growth by chemical vapour deposition. *J. Phys. D: Appl. Phys.* **2015**, *48*, 435303.
(30) *Casting design and performance*; ASM International, 2009.
(31) Marsden, A. J.; Phillips, M.; Wilson, N. R. Friction force microscopy: a simple technique for identifying graphene on rough substrates and mapping the orientation of graphene grains on copper. *Nanotechnology* **2013**, *24* (25), 255704.
(32) Fan, Y.; He, K.; Tan, H.; Speller, S.; Warner, J. H. Crack-Free Growth and Transfer of Continuous Monolayer Graphene Grown on Melted Copper. *Chem. Mater.* **2014**, *26* (17), 4984−4991.
(33) Nanda, K. K.; Sahu, S. N.; Behera, S. N. Liquid-drop model for the size-dependent melting of low-dimensional systems. *Phys. Rev. A: At., Mol., Opt. Phys.* **2002**, *66* (1), 013208.
(34) Surhone, L. M., Timpledon, M. T.; Marseken, S. F., Eds. *Planck's Law: Black Body, Radiance, Electromagnetic Radiation, Wavelength*; Betascript Publishing, 2010.

https://doi.org/10.1021/acsmaterialsau.1c00047
ACS Mater. Au 2022, 2, 79−84